Synthesis and Characterization of $Fe_3O_4@Gd_2O_3:Eu^{3+}$ Hollow Spheres with Superior Luminescence and Magnetic Properties

Fu Wenming Li Wang Wang Jun

Faculty of Science, Ningbo University, Ningbo, Zhejiang 315211, *China*

Abstract Multifunctional $Fe_3O_4@Gd_2O_3:Eu^{3+}$ hollow nanospheres are prepared via a urea-based homogeneous precipitation method. The multifunctional layers are designed to a shell-shell structure to avoid the magnetic nanoparticles clustering. Scanning electron microscope (SEM) and transmission electron microscope (TEM) images indicate that the as-obtained $Fe_3O_4@Gd_2O_3:Eu^{3+}$ sample consists of uniform nanospheres with an average diameter of 390 nm, and the thicknesses of magnetic and fluorescent layers are about 55 nm and 15 nm, respectively. The shell thickness and the size of the hollow nanospheres can easily be controlled via adjusting the concentration of raw materials and the size of silica template. The sample of $Fe_3O_4@Gd_2O_3:Eu^{3+}$ shows high saturation magnetization of 17.1 emu/g and strong red emission under ultraviolet excitation, which may be applied in targeted therapy, immune detection, magnetic separation, luminescence detection and so on. This synthesis route is of great significance in the controllable synthesis of other multifunctional hollow nanospheres as well.

Key words materials; luminescence; magnetic; homogeneous precipitation; shell-shell structure

OCIS codes 160.3820; 160.4236; 300.6280

荧光磁性$Fe_3O_4@Gd_2O_3:Eu^{3+}$空心球的制备与表征

付文明 李 旺 王 军

宁波大学理学院, 浙江 宁波 315211

摘要 通过尿素均匀沉淀法合成了荧光磁性$Fe_3O_4@Gd_2O_3:Eu^{3+}$纳米空心球,并且设计了一种壳-壳结构。利用模板法合成的这种壳-壳结构很好地避免了磁性纳米粒子的凝聚。扫描电子显微镜(SEM)和透射电子显微镜(TEM)测试结果表明,得到的$Fe_3O_4@Gd_2O_3:Eu^{3+}$空心球直径均约为390 nm,并且磁性层和荧光层的厚度分别约55 nm和15 nm。壳的厚度和空心纳米球的尺寸可以很容易地通过调整原料的浓度和氧化硅模板的尺寸来控制。所制备的$Fe_3O_4@Gd_2O_3:Eu^{3+}$空心球表现出较高的饱和磁化强度(17.1 emu/g),在紫外线的激发下发出较强的红光。这种特征使它完全可以应用于靶向治疗、免疫检测、磁性分离、荧光追踪等方面。该合成路线对其他多功能纳米空心球的可控合成也具有重要的意义。

关键词 材料; 荧光性; 磁性; 均相沉淀; 壳-壳结构

中图分类号 O160 **文献标识码** A

doi: 10.3788/CJL201643.0106006

1 Introduction

The last decade has witnessed the blossom of multifunctional mesoporousand hollow nanomaterials due to their wide range of biomedical applications in fluorescent labeling, drug delivery and molecular imaging[1-4]. Multifunctional

收稿日期: 2015-09-06; **收到修改稿日期**: 2015-09-30

基金项目: 国家自然科学基金(11474174)、浙江省自然科学基金(LY14E020002)、宁波市自然科学基金(2015A610001)、宁波大学学生研究与创新机计划和王宽诚基金

作者简介: 付文明(1987—),男,硕士研究生,主要从事荧光磁性纳米材料,锂离子电池等方面的研究。

E-mail: cassy0606@126.com

导师简介: 王 军(1969—),男,博士,教授,主要从事磁性纳米材料及其应用等方面的研究。

E-mail: wjnaf@ustc.edu(通信联系人)

mesoporous and hollow nanomaterials exhibit unique physicochemical properties, such as fluorescence, magnetism, catalyst[5-6]. Up to now, a large amount of research has focused on the synthesis and characterization of inorganic[7-9], organic[10], and inorganic/organic hybrid[11] nanomaterials. Rare-earth (RE) ions doped gadolinium oxide (Gd_2O_3) nanoparticles, which present a combination of favorable luminescent and magnetic properties, can serve as promising multifunctional materials. Recently, Tian *et al*.[12] reported the synthesis of rare-earth-doped Gd_2O_3 hollow nanospheres and investigated their up-conversion, magnetic, as well as drug adsorption and release properties. Mohapatra *et al*.[6] reported the synthesis of $CoFe_2O_4$@m-SiO_2 hollow nanoparticles and investigated their targeted co-delivery of cisplatin-pemetrexed and MR imaging. The results indicated that such material could serve as potential candidate for optical/MR imaging and drug delivery. However, the synthesis of luminescent hollow nanospheres with high magnetism remains a challenge. We choose magnetic iron oxide and Gd_2O_3:Eu^{3+}as the shell to synthesize multifunctional hollow spheres[13-16].

On the other hand, increasing endeavors have been paid to control the size of spherical diameter and the thickness of the shell, which may expand the potential applications of such materials[17-18]. The possibility of modifying the inner and outer edges and surfaces can also enhance the advantageous properties of hollow spheres[19]. Here, a hollow sphere with shell-shell structure is designed and template method to is used fabricate the shell-shell structure. The as-prepared Fe_3O_4@Gd_2O_3:Eu^{3+} hollow nanospheres exhibit superior luminescence and magnetic properties. The products contain a silica core, magnetic and fluorescent shell, the size of core and the thickness of layers can be easily controlled. This shell-shell structure can also prevent magnetic nanoparticles from aggregating.

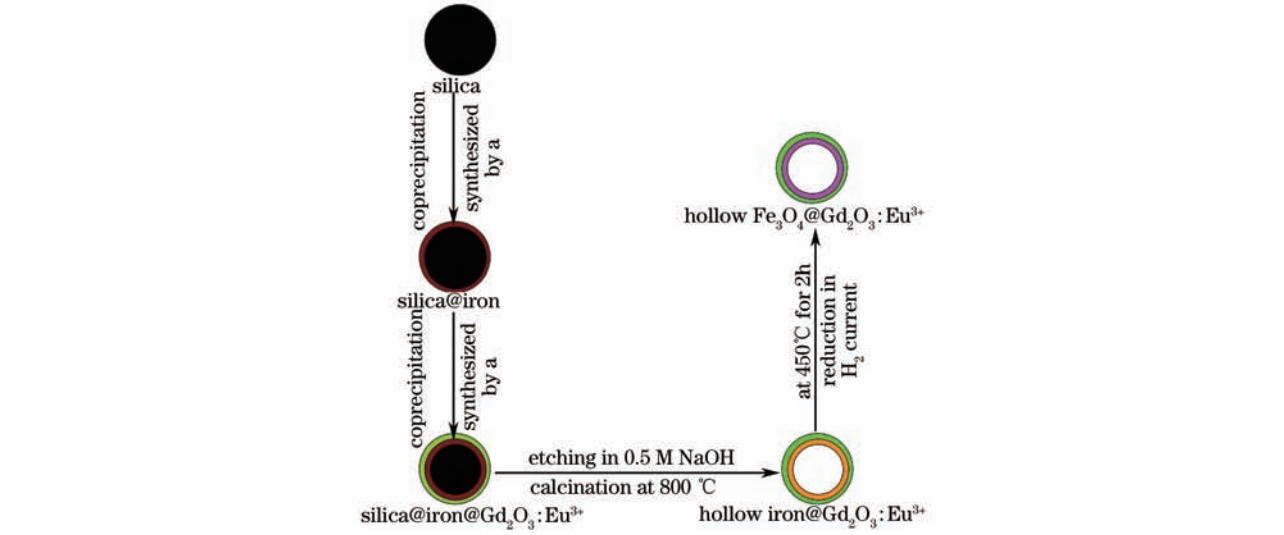

Fig.1 Schematic illustration of the preparation of Fe_3O_4@Gd_2O_3:Eu^{3+} hollow nanospheres

Figure 1 illustrates the detailed synthesis strategy of Fe_3O_4@Gd_2O_3:Eu^{3+}sample. The main steps of this approach involve synthesis of monodisperse SiO_2 templates, installation of inorganic seeds, growth and formation of inner or outer inorganic shells. Firstly, the uniform, monodisperse silica nanospheres (~250 nm) were synthesized and the silica@iron spheres were fabricated via a homogeneous precipitation route. Secondly, Silica@iron@Gd_2O_3:Eu^{3+} spheres were assembled in the way of homogeneous precipitation method. Finally, the hollow mesoporous iron@Gd_2O_3:Eu^{3+} spheres are fabricated via a sacrificial template route and reduced by H_2 current. Compared with coating the other magnetic particles with Silica, the surface of Fe_3O_4 particles modified by negatively charged groups exhibits a colossal volume to encapsulate drugs, superb monodispersity, and high uniformity.

The formation process, structure, luminescence and magnetic properties of the obtained double-deck hollow spheres are illustrated in detail. Our work may open new possibilities to synthesize other multifunctional hollow spheres with shell-shell architectures, which are believed to be important for the advancement of novel drug delivery carriers and nanomedicine.

2 Experiment

2.1 Materials

$Gd(NO_3)_3 \cdot 6H_2O$ (AR, 99.0%, mass fraction) and $Eu(NO_3)_3 \cdot 6H_2O$ (≥99.9%) were purchased from Aladdin Chemistry Co. Ltd. $Fe(NO_3)_3 \cdot 9H_2O$ (≥98.5%), $CO(NH_2)_2$ (≥99.0%) and NaOH (AR, 96%) were purchased from Sinopharm Chemical Reagent Co. Ltd. All the reagents were used without any further purification.

2.2 Preparation of Silica@iron composite spheres

The synthesis procedure of Silica@iron composite sphere involves: 1) preparation of uniform silica balls (250 nm)[20]; 2) preparation of Silica@iron spheres via a urea based homogeneous precipitation approach. The synthesis procedures are as follows: 1.20 g of SiO_2 spheres was dispersed in 100 mL of deionized water with ultrasound. Then, 0.21 g of $Fe(NO_3)_3 \cdot 9H_2O$ and 0.29 g of $CO(NH_2)_2$ were added in the solution. The mixture (100 mL) was stirred mildly at a constant temperature (90 ℃) for 4 h for a complete precipitation.

2.3 Preparation of Fe_3O_4@Gd_2O_3:5%Eu^{3+} hollow spheres

Eu^{3+}-doped Gd_2O_3 hollow nanospheres were synthesized by the same synthesis procedure: 1.20 g silica@iron sample was added to the mixed solution [6 g $CO(NH_2)_2$, 100 ml H_2O, 2 mmol of $Gd(NO_3)_3$ and 0.1 mmol of $Eu(NO_3)_3$ for Gd_2O_3: 5% Eu^{3+}]. The Mixed solution in advance was also stirred mildly at a constant temperature of 90 ℃ for 4 h. The silica cores were etched by immersing the silica@iron@Gd_2O_3:Eu^{3+}spheres in 200 mL of 20% NaOH. The shell-shell samples were collected by centrifugation. Then, these powders were obtained through heat treatment at 800 ℃ for 2 h in air at a heating rate of 10 ℃/min. Finally, in order to enhance the magnetism of the iron@Gd_2O_3:Eu^{3+} hollow spheres, the particles were maintained at 450 ℃ for 2 h under a hydrogen atmosphere in the fixed-bed reactor. After the completion of the reduction process, the sample was protected at room temperature in the flowing-inert gas for 12 h.

2.4 Characterization

X-ray diffraction (XRD) patterns of the sample were provided by Brucker-D8 ADVANCE XRD with Cu-K_α radiation. Transmission electron microscope (TEM, JEM-2100F) and scanning electron microscope (SEM, SU-70) equipped with an energy-dispersive X-ray spectrum spectrometer (EDX) were used to analyze the morphology and elements of the samples. The N_2 adsorption/desorption isotherm data from micromeritics (ASAP 2020M) measurement was used to analyze the Brunauer-Emmett-Teller (BET) surface area and pore size distribution. A cary eclipse fluorescence spectrophotometer was used to record the photoluminescence (PL) excitation and emission spectra, and a 150 W xenonlamp was equipped on the cary eclipse Fluorescence spectrophotometer as the excitation source. A lecroy wave runner 6100 digital oscilloscope (1 GHz) was used to obtain the luminescence decay curves, and atunable laser (pulse width=4 ns, gate=50 ns) on the lecroy wave runner 6100 digital oscilloscope was used as the excitationsource (contimuum sunlite OPO). The magnetic properties were measured by a vibrating sample magnetometer of physical property measurement system (PPMS, quantum design).

3 Results and discussion

SEM and TEM images of colloidal SiO_2 particle template are displayed in Fig.2 (a) and (b), respectively. Obviously, the as-synthesized silica spheres are monodisperse and show a narrow size distribution around 250 nm in diameter. The results of Fig.2 (c) and (d) present uniform Silica@iron spheres with flocculent surfaces. Their diameters of Silica@iron solid spheres is about 355 nm, and the thickness of iron layer is approximately 55 nm.

Figure 3 (a) and (b) give the SEM and TEM images of silica@iron@Gd_2O_3:Eu^{3+} spheres. The SEM images show that the samples consist of well-preserved, uniform nanospheres. And obvious change in particle size occurs on conversion of the shell to Gd_2O_3:Eu^{3+} from flocculent to mesoporous solid spheres, which can be found in the TEM image. The images show that the nanospheres core-shells structure with a diameter of 390 nm, and thickness of the layer approximately 70 nm .

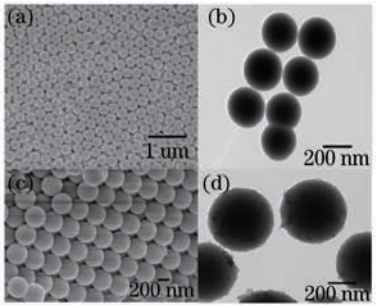

Fig.2 SEM (a) and TEM (b) images of SiO_2 nanospheres. SEM (c) and TEM (d)images of Silica@iron composite nanospheres

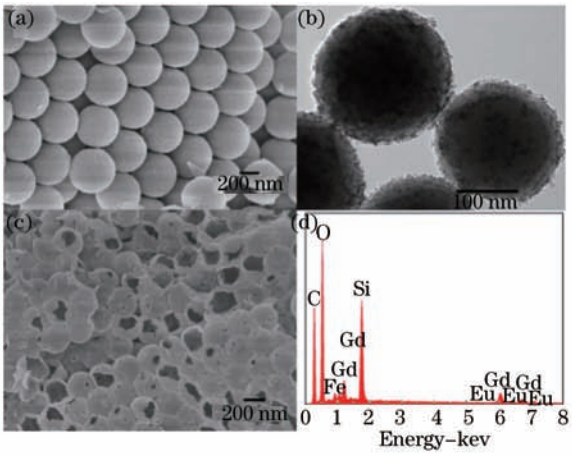

Fig.3 SEM image (a) and TEM image (b) of silica@iron@Gd_2O_3:Eu^{3+} spheres. SEM image (c) of Fe_3O_4@Gd_2O_3:Eu^{3+} hollow spheres with SiO_2 fully etched and dealt with ultrasound. (d) EDX result of Fe_3O_4@Gd_2O_3:Eu^{3+} hollow spheres

By immersing the products in sodium hydroxide solution, the silica cores were dissolved by alkaline and the remainder shells were collected by centrifugation. SEM image in Fig.3 (c) shows the hollow spheres with SiO_2 fully etched and dealt with ultrasound. The broken particles clearly reveal that the hollow structures are obtained after products were dealt with ultrasound for some time. EDX spectra in Fig.3(d) recorded on the Fe_3O_4@Gd_2O_3:Eu^{3+} spheres indicate the presence of Fe, Gd, Eu, Si, and O in nanospheres, further confirming the composition of the sample.

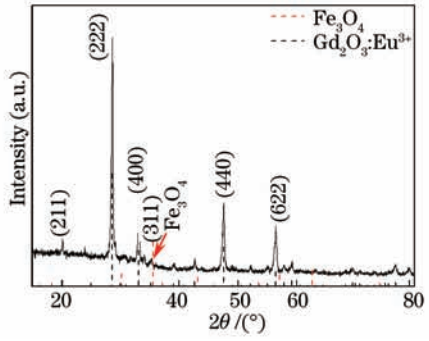

Fig.4 X-ray diffraction pattern of Fe_3O_4@Gd_2O_3:Eu^{3+} hollow nanoparticles with representative index on typical peaks

Figure 4 shows the XRD patterns of these hollow nanospheres reduced by H_2 current. It is clear that the diffraction peaks located at 2θ=28.6°, 33.1°, 47.5°, and 56.4° are assigned to the (222), (400), (440), and (622) lattice planes of cubic Gd_2O_3, in accordance with the standard data (JCPDS card No. 43-1014). In addition, at the positions marked by arrows, a set of very weak diffraction peaks assigned to the cubic phase of Fe_3O_4 (JCPDS card No.19-0629) were detected. No other crystalline impurities were detected, indicating the well crystallization of the products.

A jump beginning is displayed at the curve of N_2 adsorption-desorption isotherms of these hollow nanoparticles at a relative pressure in the range P/P_0=0.2~0.3 [Fig.5(a)], which suggests that the hollow spheres have the uniform mesoporosity. The N_2 adsorption-desorption isotherms can belong to type-IV. Meanwhile, a H1-type hysteresis loop

appears in its isotherm, which represents narrow pore distributions. The pore size is calculated to be 4.8 nm and the BET surface area is 9.4 m^2/g [Fig.5(b)]. It is important for drug delivery that the particular structure of the magnetic and luminescent hollow nanomaterials with hollow cavities and mesostructured pore wall.

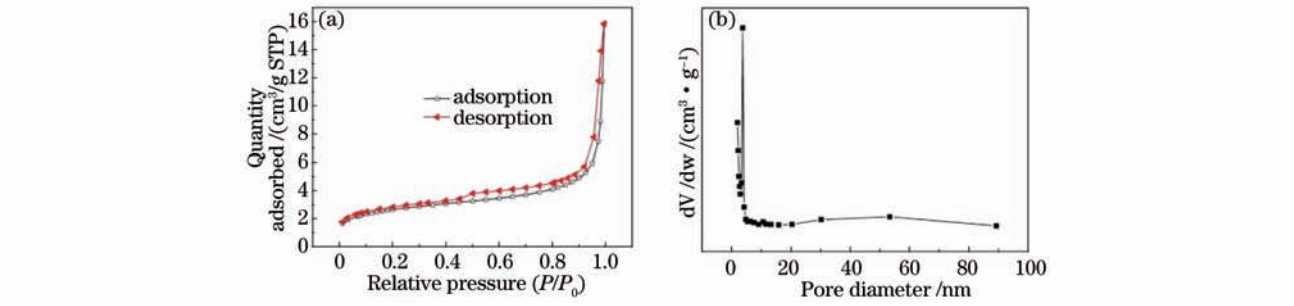

Fig.5 N_2 adsorption-desorption isotherms (a) and pore diameter distribution of $Fe_3O_4@Gd_2O_3:Eu^{3+}$ hollow nanospheres (b)

A vibrating sample magnetometer is used to measure the magnetic properties of $Fe_3O_4@Gd_2O_3:Eu^{3+}$ hollow nanospheres at room temperature. As displayed in Fig.6, the sample presents a saturation magnetization (M_S) of 17.1 emu/g and a relatively low coercivity not higher than 15 Oe (13.23 Oe) at room temperature. It should be noted that the hollow nanoparticles exhibit superparamagnetic behavior in Fig.6. Compared with the saturation magnetization of the magnetic and luminescent fluoride nanorattles such as $Fe_3O_4@SiO_2@\alpha$-NaYF/Yb (1.28 emu/g)[21], our sample can be more easily directed by an external magnetic field to a specific target for a variety of biological applications. Remarkably, through increasing thickness of magnetic shell with the times of coating, the saturation magnetization of products will be enhanced.

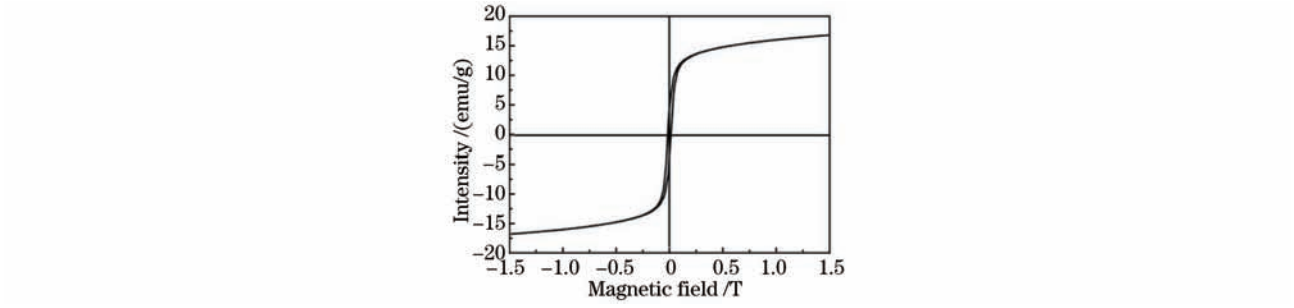

Fig.6 Room-temperature (300 K) magnetic hysteresis loops of $Fe_3O_4@Gd_2O_3:Eu^{3+}$ hollow nanospheres

The fluorescence spectra of the $Fe_3O_4@Gd_2O_3:Eu^{3+}$ hollow samples are shown in Fig.7 (a). The excitation spectrum include a strong, broad band at about 243 nm and some weak, sharp lines in the longer-wavelength region, which are due to the charge-transfer band (CTB) between the O^{2-} and Eu^{3+} ions and the f-f transitions of the Gd^{3+} and Eu^{3+} ions, respectively. Upon excitation into the CTB of Eu^{3+} ions at 243 nm, the emission spectrum exhibits six groups of emission lines (580,589, 610, 617, 654, 700 nm), which are ascribed to the $^5D_0-^7F_J$ (J= 0, 1, 2, 2, 3, 4) transitions of the Eu^{3+} ions. The decay curve for the luminescence of Eu^{3+} ($^5D_0-^7F_2$, 610 nm) in Gd_2O_3 host lattice is presented in Fig.7 (b). Upon excitation into the CTB of Eu^{3+} ions at 243 nm, the luminescence decay curve of $Gd_2O_3:Eu^{3+}$ can be well fitted to a single-exponential

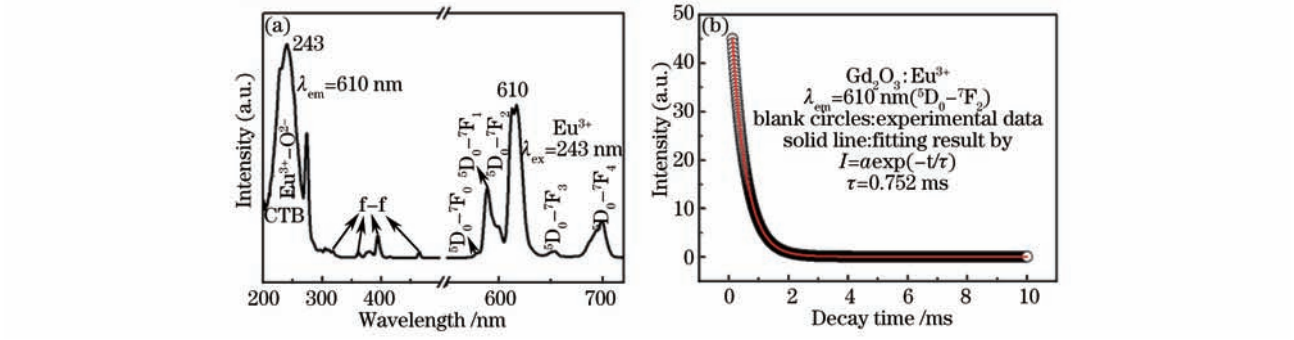

Fig.7 Excitation and emission spectra (a) and decay curve of as-synthesized $Fe_3O_4@Gd_2O_3:Eu^{3+}$ hollow nanospheres (b)

function, and the lifetime of Eu^{3+} is determined to be 0.752 ms.These results are basically in agreement with other Eu^{3+}-Gd_2O_3 systems in the previous reports[22-25].

4 Conclusion

The feasible route to prepare uniform multifunctional shell-shell structure has been demonstrated, which can combine the advantages of these single materials and avoid nanoparticles clustering. This strategy is adopted to synthesize multifunctional $Fe_3O_4@Gd_2O_3:Eu^{3+}$ hollow nanospheres with excellent magnetic (17.1 emu/g) and luminescent properties by a layer-by-layer method. The $Fe_3O_4@Gd_2O_3:Eu^{3+}$ hollow nanospheres can be used as the carriers for drug delivery. This work can provide a promising route to design and synthesize multifunctional optomagnetic microspheres and other multifunctional hollow spheres, which can be used for biomedical fields, fluorescent labeling, molecular imaging and catalysis.

References

1 Wu H X, Zhang S J, Zhang J M, *et al*.. A hollow-core, magnetic, and mesoporous double-shell nanostructure: *In-situ* decomposition/reduction synthesis, bioimaging, and drug-delivery properties[J]. Adv Funct Mater, 2011, 21(10): 1850-1862.

2 Sun L, Zang Y, Sun M D, *et al*.. Synthesis of magnetic and fluorescent multifunctional hollow silica nanocomposites for live cell imaging [J]. J Colloid Interface Sci, 2010, 350(1): 90-98.

3 Yang D M, Li C X, Lin J, *et al*.. Hollow structured upconversion luminescent $NaYF_4:Yb^{3+}$, Er^{3+} nanospheres for cell imaging and targeted anti-cancer drug delivery[J]. J Biomaterials, 2013, 34(5): 1601-1612.

4 Tian G, Gu Z J, Liu X X, *et al*.. Facile fabrication of rare-earth-doped Gd_2O_3 hollow spheres with upconversion luminescence, magnetic resonance, and drug delivery properties[J]. J Phys Chem C, 2011, 115(48): 23790-23796.

5 Hu J, Chen M, Fang X S, *et al*.. Fabrication and application of inorganic hollow spheres[J]. Chem Soc Rev, 2011, 40(11): 5472-5491.

6 Mohapatra S, Rout S R, Narayan R, *et al*.. Multifunctional mesoporous hollow silica nanocapsules for targeted co-delivery of cisplatin-pemetrexed and MR imaging[J]. Dalton Trans, 2014, 43(42): 15841-15850.

7 Chen Y, Chen H G, Zhang S G, *et al*.. Multifunctional mesoporous nanoellipsoids for biological bimodal imaging and magnetically targeted delivery of anticancer drugs[J]. Adv Funct Mater, 2011, 21(2): 270-278.

8 Zhang T R, Ge J P, Hu Y X, *et al*.. Formation of hollow silica colloids through a spontaneous dissolution-regrowth process[J]. Angew Chem, 2008, 120(31): 5890-5895.

9 Cheng T L, Li S G, Zhou G Y, *et al*.. Relation between power fraction in the core of hollow-core photonic crystal fibers and their bandgap property[J]. Chinese J Lasers, 2007, 2(2): 249-254.
程同蕾, 李曙光, 周桂耀, 等. 空芯光子晶体光纤纤芯中的功率分数及其带隙特性[J]. 中国激光, 2007, 2(2): 249-254.

10 Li B, Yang X, Xia L, *et al*.. Hollow microporous organic capsules[J]. Sci Rep, 2013: 3.

11 Rawolle M, Niedermeier M A, Kaune G, *et al*.. Fabrication and characterization of nanostructured titania films with integrated function from inorganic-organic hybrid materials[J]. Chem Soc Rev, 2012, 41(15): 5131-5142.

12 Tian G, Gu Z J, Liu X X, *et al*.. Facile fabrication of rare-earth-doped Gd_2O_3 hollow spheres with upconversion luminescence, magnetic resonance, and drug delivery properties[J]. J Phys Chem C, 2011, 115(48): 23790-23796.

13 Deng Y H, Qi D W, Deng C H, *et al*.. Super paramagnetic high-magnetization microspheres with an $Fe_3O_4@SiO_2$ core and perpendicularly aligned mesoporous SiO_2 shell for removal of microcystins[J]. J Am Chem Soc, 2008, 130(1): 28-29.

14 Cui Xiaoxia, Gao Fei, Hou Chaoqi, *et al*.. Synthesisi and optical properties of neodymium-doped lanthannum fluoride nano-laser materials [J]. Chinese J Lasers, 2013, 40(6): 0606003.
崔晓霞, 高 飞, 候超奇, 等. 氟化镧掺钕纳米激光材料的制备及光学性能[J]. 中国激光, 2013, 40(6): 0606003.

15 Fujishiro F, Sekimoto R, Hashimoto T. Photoluminescence properties of $CuLa_{1-x}Ln_xO_2$ (Ln: lanthanide)-intense and peculiar luminescence from Ln^{3+} at the site with inversion symmetry[J]. J Lumin, 2013, 133: 217-221.

16 Kang X J, Cheng Z Y, Yang D M, *et al*.. Design and synthesis of multifunctional drug carriers based on luminescent rattle-type mesoporous silica microspheres with a thermosensitive hydrogel as a controlled switch[J]. Adv Funct Mater, 2012, 22(7): 1470-1481.

17 Cong Y H, Wang G L, Xiong M H, *et al*.. A facile interfacial reaction route to prepare magnetic hollow spheres with tunable shell thickness

[J]. Langmuir, 2008, 24(13): 6624-6629.

18 Yang J, Li C X, Cheng Z Y, *et al*.. Size-tailored synthesis and luminescent properties of one-dimensional Gd_2O_3:Eu^{3+} nanorods and microrods[J]. J Phys Chem C, 2007, 111(49): 18148-18154.

19 Jia G, Liu K, Zheng Y H, *et al*.. Highly uniform $Gd(OH)_3$ and Gd_2O_3:Eu^{3+} nanotubes: facile synthesis and luminescence properties[J]. J Phys Chem C, 2009, 113(15): 6050-6055.

20 Stöber W, Fink A, Bohn E. Controlled growth of monodisperse silica spheres in the micron size range[J]. Colloid Interface Sci, 1968, 26 (1): 62-69.

21 Zhang F, Braun G B, Pallaoro A, *et al*.. Mesoporous multifunctional upconversion luminescent and magnetic "nanorattle" materials for targeted chemotherapy[J]. Nano Lett, 2011, 12(1): 61-67.

22 Qu X S, Yang H K, Moon B K, *et al*.. Preparation and photoluminescence properties of Gd_2O_3:Eu^{3+} inverse opal photonic crystals[J]. J Phys Chem C, 2010, 114(47): 19891-19894.

23 Sun W Z, Pang R, Li H F, *et al*.. Synthesis and photoluminescence properties of novel red-emitting $Ca_{14}Mg_2(SiO_4)_8$:Eu^{3+}/Sm^{3+} phosphors [J]. J Rare Earths, 2015, 33(8): 814-819.

24 Li H F, Zhao R, Jia Y L, *et al*.. $Sr_{1.7}Zn_{0.3}CeO_4$:Eu^{3+} novel red-emitting phosphors: synthesis and photoluminescence properties [J]. Appl Mater Interfaces, 2014, 6(5): 3163-3169.

25 Wang Jinxian, Che Hongrui, Dong Xiangting, *et al*.. Fabrication and characterization of Gd_2O_3:Eu^{3+} luminescent nanofibers via electrospining [J]. Acta Optica Sinica, 2010, 2(2): 473-479.

王进贤, 车红锐, 董相廷, 等. 静电纺丝技术制备Gd_2O_3:Eu^{3+}发光纳米纤维与表征[J]. 光学学报, 2010, 2(2): 473-479.

栏目编辑：张浩佳